INSTITUTE OF PHYSICS PUBLISHING JOURNAL OF PHYSICS: CONDENSED MATTER

J. Phys.: Condens. Matter **16** (2004) S293–S299 PII: S0953-8984(04)66987-6

N^+ ion-implantation-induced defects in ZnO studied with a slow positron beam

Z Q Chen[1,3], T Sekiguchi[2], X L Yuan[2], M Maekawa[1] and A Kawasuso[1]

[1] Japan Atomic Energy Research Institute, 1233 Watanuki, Takasaki, Gunma 370-1292, Japan
[2] Nanomaterials Laboratory, National Institute for Materials Science, 1-2-1 Sengen, Tsukuba, Ibaraki 305-0047, Japan

E-mail: chenzq@taka.jaeri.go.jp

Received 31 July 2003
Published 22 December 2003
Online at stacks.iop.org/JPhysCM/16/S293 (DOI: 10.1088/0953-8984/16/2/035)

Abstract

Undoped ZnO single crystals were implanted with multiple-energy N^+ ions ranging from 50 to 380 keV with doses from 10^{12} to 10^{14} cm^{-2}. Positron annihilation measurements show that vacancy defects are introduced in the implanted layers. The concentration of the vacancy defects increases with increasing ion dose. The annealing behaviour of the defects can be divided into four stages, which correspond to the formation and recovery of large vacancy clusters and the formation and disappearance of vacancy–impurity complexes, respectively. All the implantation-induced defects are removed by annealing at 1200 °C. Cathodoluminescence measurements show that the ion-implantation-induced defects act as nonradiative recombination centres to suppress the ultraviolet (UV) emission. After annealing, these defects disappear gradually and the UV emission reappears, which coincides with positron annihilation measurements. Hall measurements reveal that after N^+ implantation, the ZnO layer still shows n-type conductivity.

1. Introduction

ZnO is becoming an attractive material for application in short-wavelength optoelectronic devices because of its wide band gap (3.4 keV) and large exciton binding energy (60 meV) [1]. However, the production of ZnO-based devices has been hindered due to the problem of doping asymmetry. It is very easy to obtain n-type ZnO, but it is rather difficult to achieve p-type conductivity.

Ion implantation is an effective way of doping in semiconductors. It has the advantage of precise control of the dopant concentration in a selected area. However, after ion implantation, a number of defects are also introduced. These defects will strongly affect the electrical

[3] Author to whom any correspondence should be addressed.

and optical properties of semiconductors. Despite extensive studies on ion implantation in ZnO [2–8], to our knowledge little attention has been paid to implantation-induced defects [3, 5, 7].

Positron annihilation spectroscopy has been proved to be a powerful tool for the study of defects in semiconductors [9]. Due to strong Coulomb repulsion from the positive ion cores, positrons are preferentially trapped by open volume-type defects. Because of the reduced electron density and the reduced annihilation rate of those positrons with high-momentum core electrons at the vacancy site, the positron lifetime will become longer, and the Doppler broadening line shape will become narrower. Observation of such differences is a clear indication of the existence of vacancy defects.

In this work, nitrogen ions were implanted into ZnO single crystals, which was expected to be a good p-type dopant. The implantation-induced defects and their recovery were studied by Doppler broadening measurements using a variable-energy slow-positron beam (0–30 keV). Hall and cathodoluminescence (CL) measurements were also performed in order to check the optical and electrical properties after implantation and annealing.

2. Experiment

Hydrothermal-grown n-type ZnO(0001) single crystals were purchased from the Scientific Production Company (SPC). N^+-implantation was performed using a 400 keV ion implanter at the Japan Atomic Energy Research Institute (JAERI). N^+ ions with seven different energies ranging from 50 to 380 keV were implanted from the zinc face to form a box-like layer of nitrogen with uniform distribution. TRIM calculation gives the box layer thickness as about 600 nm [10]. The implantation dose ranged from 10^{12} to 10^{14} cm^{-2}. After implantation, the samples were annealed in the temperature range from 20 to 1200 °C for 30 min in a nitrogen atmosphere.

Doppler broadening spectra were analysed using S- and W-parameters, which are defined as the ratio of the central region (511 ± 0.77 keV) and the wing region (511 ± 3.4 to 511 ± 6.8 keV) to the total area of 511 keV annihilation peak, respectively. A higher S-parameter (lower W-parameter) than that of the defect-free state is therefore an indication of the existence of vacancy defects.

CL was measured at room temperature using a modified scanning electron microscope (Topcon DS-130) [11]. The electron beam energy was 5 keV and beam current was about 3 nA. Hall measurement was performed using the van der Pauw method [12].

3. Results and discussion

Figure 1 shows the S-parameter as a function of positron incident energy (S–E curve) for the as-grown and N^+-implanted ZnO. In this paper, the S-parameters are normalized to the value in the unimplanted bulk ZnO. In the as-grown sample, the S-parameter decreases from about 1.12 to the bulk value with increasing positron energy. This reflects the change of the positron state from surface to the bulk ($E > 20$ keV). After N^+ implantation, the S-parameter shows a considerable increase. There is a plateau in the region of 5–13 keV, and the S-parameter in this region increases with ion dose. This increase in the S-parameter is obviously due to positron trapping by vacancies introduced by implantation.

Considering the implantation profile and diffusion of positrons, the S-parameter at a given positron incident energy may be a combination of several annihilation states:

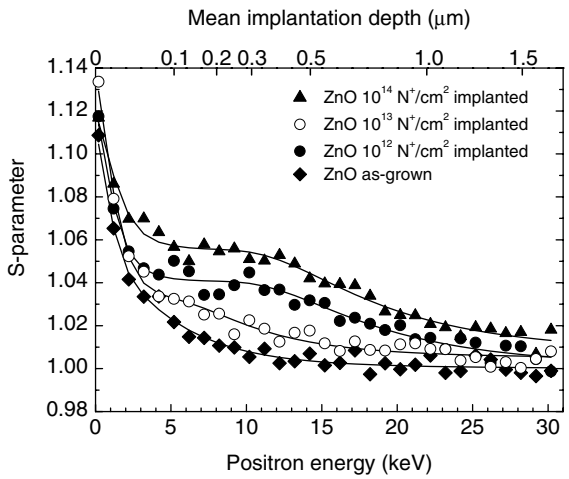

Figure 1. *S–E* curve measured for the ZnO implanted with N^+ ions at different doses. The curves are obtained from the VEPFIT analyses.

$$S(E) = S_s F_s(E) + \sum_{i=1}^{n} S_i F_i(E) \tag{1}$$

$$F_s(E) + \sum_{i=1}^{n} F_i(E) = 1 \tag{2}$$

where S_s and S_i are the S-parameters corresponding to the surface and ith layers. The S–E curve is then analysed by the VEPFIT program [13] by resolving the following one-dimensional diffusion equation:

$$D_+ \frac{d^2}{dz^2} n(z) - \kappa_{\text{eff}}(z) n(z) + P(z, E) = 0 \tag{3}$$

where $P(z, E)$ is the positron implantation profile, D_+ is the positron diffusion coefficient and $\kappa_{\text{eff}}(z)$ is the effective escape rate of positrons from the diffusion process. From VEPFIT analysis, the damage layer thickness is about 600 nm. This agrees very well with the TRIM calculation of the vacancy profile.

Figure 2 presents the S-parameter in the damage layers as a function of ion dose. The S-parameter increases continuously with ion dose, and attains nearly 1.06 after 10^{14} N^+ cm^{-2} implantation. The increase in both vacancy size and vacancy concentration may cause the increase in the S-parameter. The W-parameter, which contains complementary information to the S-parameter, may give us some further hints. We plot the change of S-parameter versus W-parameter in the inset of figure 2 for all the as-grown and implanted samples, and the S–W plot shows a nearly straight line. This means that the defect species do not change with increasing ion dose, only the defect concentration increases. From our previous study of the electron-irradiation-induced defects in ZnO, the S-parameter for a zinc monovacancy (S_d) is only about 1.018. Therefore, we may estimate that the predominant defects in our implanted ZnO layer are vacancy clusters, i.e. larger than monovacancies. But we cannot rule out that a small number of monovacancies are also produced at the same time. They might coexist with vacancy clusters.

The effect of annealing on the S–E curves for the implanted sample with the highest dose (10^{14} cm^{-2}) is shown in figure 3. Only some curves at selected temperatures are presented in

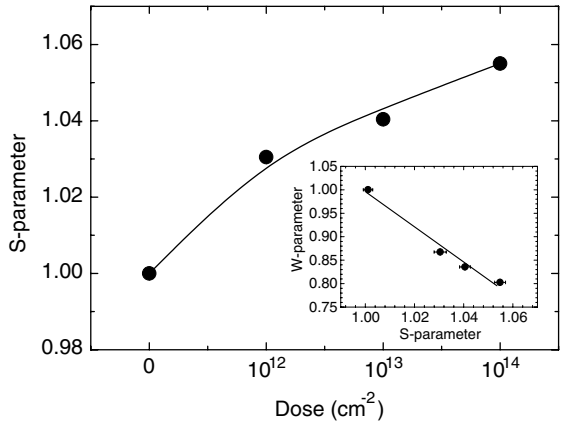

Figure 2. *S*-parameter in the implanted layers as a function of N^+ ion dose. The inset shows the change of *S*-parameter versus *W*-parameter for the as-grown and implanted samples.

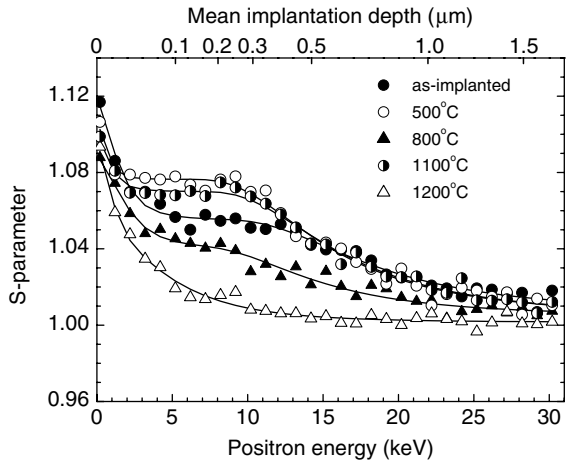

Figure 3. *S*–*E* curve measured for the implanted ZnO with dose of 10^{14} cm^{-2} after annealing at different temperatures. The curves are obtained from the VEPFIT analyses. The annealing was performed in a nitrogen ambient for 30 min.

order to avoid overlap with each other. Figure 4 shows the VEPFIT analysed *S*-parameter in the damage layer as a function of annealing temperature. The annealing behaviour shows four stages. In stage I (20–500 °C), the *S*-parameter increases with annealing temperature, then it begins to decrease in stage II (500–800 °C). In stage III (800–1100 °C), the *S*-parameter increases again, and finally in stage IV (1100–1200 °C) it recovers to that of the un-implanted state.

The increase in the *S*-parameter in stage I might be due to the migration and subsequent agglomeration of vacancies into larger vacancy clusters, as these are energetically more favourable states. The subsequent decrease in the *S*-parameter in stage II can be attributed to the recovery of these vacancy clusters.

It is interesting to note that the *S*-parameter does not show complete recovery in stage II. After annealing at 800 °C, it decreases to 1.037, but this is still much higher than the bulk value. This means that some vacancy clusters still remain at 800 °C. Further annealing in stage

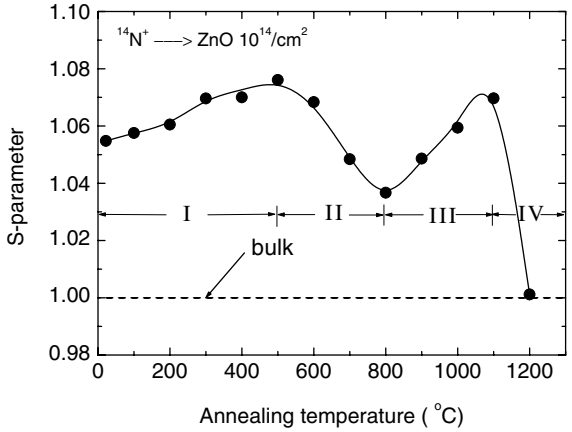

Figure 4. *S*-parameter in the implanted layers as a function of annealing temperature for the N^+-implanted ZnO. The annealing was performed in a nitrogen ambient for 30 min.

III reveals that the *S*-parameter increases again, and reaches 1.07 at 1100 °C. This abnormal annealing behaviour suggests that some new positron trapping centres appear. Actually for the ZnO implanted by some other ions, like Al^+, we did not observe the annealing stage III and IV, and all the defects were annealed out at 800–900 °C, i.e. the annealing finished in stage II. This means that the last two annealing stages in N^+-implanted ZnO might be due to the nitrogen impurities. From a recent calculation of the compensation mechanism in ZnO [14], the nitrogen acceptors will interact with various defects to form defect complexes. Therefore, the increase in the *S*-parameter in stage III in the N^+-implanted ZnO might be due to the formation of nitrogen-related vacancy complexes. The nitrogen impurities which replaced oxygen will cause the increase in the *S*-parameter if they are near the vacancies. This is because the oxygen impurity near the vacancy generally causes a low *S*-parameter due to the high probability of positron annihilation with the high-momentum core electrons of oxygen. This phenomenon is well known in the oxygen-implanted Si layers where the *S*-parameter for the vacancy–oxygen complexes is even lower than the bulk value [15]. The formation of nitrogen–vacancy complexes has also been observed in many other semiconductors, for example in Si [16, 17], diamond [18] and SiC [19, 20].

When the implanted sample was annealed at 1200 °C, the *S*-parameter drops to the value of the bulk state. This means that all the implantation-induced vacancies are removed after this high-temperature annealing.

The CL measurements for some selected samples are shown in figure 5. In the unimplanted sample there is a very weak band edge ultraviolet (UV) emission, which is due to the recombination of free excitons in ZnO. This weak UV emission might be due to the existence of nonradiative recombination centres in the as-grown materials. After N^+ implantation at a dose of 10^{14} cm^{-2}, the small UV emission peak disappears completely. This means that ion-implantation-induced defects act as nonradiative recombination centres and suppress the UV emission. After annealing at 500 °C, the UV emission reappeared, but the intensity is still very small. After the further annealing at 1200 °C, the UV emission shows full recovery, and it is even enhanced compared with the unimplanted state. This indicates that the implantation-induced defects are fully removed by annealing. For the as-grown sample, we find that after annealing at the same temperature (1200 °C) the UV emission also increases. Thus the enhancement of UV emission might be due to the reduction of nonradiative defects in the as-grown ZnO through annealing.

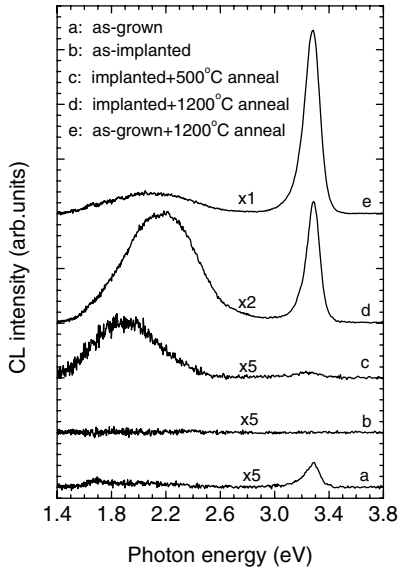

Figure 5. CL measurements of as-grown and N^+-implanted ZnO before and after annealing.

Table 1. Hall measurements of free electron concentration n_e, resistivity ρ and electron mobility μ in the as-grown and N^+-implanted (10^{14} cm^{-2}) ZnO after annealing.

Sample	ρ (Ω cm)	n_e (cm^{-3})	μ (cm^2 V^{-1} s^{-1})
As-grown	1.7×10^4	5.7×10^{12}	66
As-grown + 1200 °C anneal	0.88	1.4×10^{17}	51
Implanted + 1200 °C anneal	0.68	1.7×10^{17}	55

The results of the Hall measurements are listed in table 1. For the as-grown sample, the resistivity is rather high, about 1.7×10^4 Ω cm. After annealing at 1200 °C, it increases to 0.88 Ω cm. This might be due to the production of donor type defects after annealing, such as the oxygen vacancy (V_O) or zinc interstitials (Zn_i). However, after N^+ implantation with a dose of 10^{14} cm^{-2} and annealing, the sample still exhibits n-type conductivity and the resistivity is nearly the same as that of the as-grown sample after annealing. This means that N^+ ion implantation does not cause p-type conversion. There are some possible reasons: one reason might be due to out-diffusion of nitrogen after the annealing at 1200 °C. Another possible reason is that nitrogen remains in the ZnO material after annealing, but is electrically inactive. This has recently been proposed by Garces *et al* [21] through electron paramagnetic resonance measurements. The nitrogen might be trapped in large vacancy complexes to become electrically inactive, as evidenced by our positron annihilation results in the annealing stages III and IV, and still remains inactive after the recovery of the vacancy defects at 1200 °C. One further possibility is that the nitrogen acceptors are over-compensated by some other donor-type defects, such as V_O, Zn_i or Zn_O, as predicted by Lee *et al* [14]. These defects may be produced during ion implantation or after high-temperature annealing, and are invisible to positrons.

4. Conclusion

Vacancy clusters are introduced by N^+ implantation in ZnO. Annealing of these vacancies shows four stages. The increase in the *S*-parameter in stage I (20–500 °C) is due to the increase in the vacancy cluster size. The later decrease in the *S*-parameter in stage II (500–800 °C) is then attributed to the partial recovery of these vacancy clusters. Formation of vacancy–impurity complexes is observed in stage III (800–1100 °C), and they are annealed out in the last stage (1100–1200 °C). The implantation-induced defects suppress the UV emission, and they are gradually removed after annealing. The N^+-implanted ZnO still shows n-type conductivity after final annealing, which might be due to the out-diffusion of nitrogen, the electrically inactive state of nitrogen or the over-compensation of the nitrogen acceptors by defects.

Acknowledgment

This work was partly supported by the Nuclear Energy Generic Crossover Research Project promoted by Ministry of Education, Culture, Sports, Science and Technology of Japan.

References

[1] Look D C 2001 *Mater. Sci. Eng.* B **80** 383
[2] Thomas B W and Walsh D 1973 *J. Phys. D: Appl. Phys.* **6** 612
[3] Sonder E, Zuhr R A and Valiga R E 1988 *J. Appl. Phys.* **64** 1140
[4] Kohiki S, Nishitani M and Wada T 1994 *J. Appl. Phys.* **75** 2069
[5] Auret F D, Goodman S A, Hayes M, Legodi M J, van Laarhoven H A and Look D C 2001 *Appl. Phys. Lett.* **79** 3074
Auret F D, Goodman S A, Hayes M, Legodi M J, van Laarhoven H A and Look D C 2001 *J. Phys.: Condens. Matter* **13** 8989
[6] Kucheyev S O, Deenapanray P N K, Jagadish C, Williams J S, Yano M, Koike K, Sasa S, Inoue M and Ogata K 2002 *Appl. Phys. Lett.* **81** 3350
Kucheyev S O, Deenapanray P N K, Jagadish C, Williams J S, Yano M, Koike K, Sasa S, Inoue M and Ogata K 2003 *J. Appl. Phys.* **93** 2972
[7] Kucheyev S O, Williams J S, Jagadish C, Zou J, Evans C, Nelson A J and Hamza A V 2003 *Phys. Rev.* B **67** 094115
[8] Wahl U, Rita E, Correia J G, Alves E and Araújo J P 2003 *Appl. Phys. Lett.* **82** 1173
[9] Krause-Rehberg R and Leipner H S 1999 *Positron Annihilation in Semiconductors, Defect Studies* (*Springer Series in Solid-State Sciences* vol 127) (Berlin: Springer)
[10] Biersack J P and Haggmark L G 1980 *Nucl. Instrum. Methods* **174** 257
[11] Sekiguchi T and Sumino K 1995 *Rev. Sci. Instrum.* **66** 4277
[12] van der Pauw L J 1958 *Philips Res. Rep.* **13** 1
[13] van Veen A, Schut H, de Vries J, Hakvoort R A and Ijpma M R 1990 *AIP Conf. Proc.* **218** 171
[14] Lee E-C, Kim Y-S, Jin Y-G and Chang K J 2001 *Phys. Rev.* B **64** 085120
[15] Uedono A, Chen Z Q, Ogura A, Ono H, Suzuki R, Ohdaira T and Mikado T 2001 *J. Appl. Phys.* **90** 6026
[16] Sawada H and Kawakami K 2000 *Phys. Rev.* B **62** 1851
[17] Adam L S, Law M E, Szpala S, Simpson P J, Lawther D, Dokumaci O and Hegde S 2001 *Appl. Phys. Lett.* **79** 623
[18] Mainwood A 1994 *Phys. Rev.* B **49** 7934
[19] Girka A I, Kuleshin V A, Mokrushin A D, Mokhov E N, Svirida S V and Shishkin A V 1989 *Sov. Phys.—Semicond.* **23** 1337
[20] Kawasuso A, Itoh H, Okada S and Okumura H 1996 *J. Appl. Phys.* **80** 5639
[21] Garces N Y, Wang L J, Giles N C, Halliburton L E, Cantwell G and Eason D B 2003 *J. Appl. Phys.* **94** 519